Asymmetric reflectance and cluster size effects in silver percolation films

Nicholas A. Kuhta,[1,*] Aiqing Chen,[2,†] Keisuke Hasegawa,[2,‡] Miriam Deutsch,[2,§] and Viktor A. Podolskiy[1,3,‖]

[1]*Department of Physics, 301 Weniger Hall, Oregon State University, Corvallis, Oregon 97331, USA*

[2]*Department of Physics, 1274 University of Oregon, Eugene, Oregon 97403, USA*

[3]*Department of Physics and Applied Physics, One University Avenue, University of Massachusetts Lowell, Lowell, Massachusetts 01854, USA*

(Received 5 August 2011; revised manuscript received 28 September 2011; published 27 October 2011)

We develop a quantitative description of giant asymmetry in reflectance, recently observed in semicontinuous metal films. The developed scaling-theory-based technique reproduces the spectral properties of semicontinuous composites, as well as provides insight into the origin of the experimentally observed loss, reflectance, and transmittance anomalies in the vicinity of the percolation threshold.

DOI: 10.1103/PhysRevB.84.165130 PACS number(s): 78.67.Sc, 42.25.Dd, 78.67.Bf, 78.66.Sq

I. INTRODUCTION

Research into the optics of semicontinuous metal-dielectric films has been enjoying sustained interest due to a unique combination of novel physics and the practical applications offered by such composites. It has been demonstrated, both theoretically and experimentally, that the electromagnetic (EM) response of these structures is dominated by a nontrivial interplay between Anderson-localized and delocalized surface plasmon polaritons.[1–3] This results in unusual optical properties that include greatly enhanced absorption, giant intensity fluctuations of local EM fields, giant local chiral response, and strongly enhanced optical nonlinearities.[4–10] In a related context, it has been recently shown that the reflectance of semicontinuous silver nanocomposites, chemically deposited on glass substrates, strongly depends on the direction of incident light.[11] In particular, the reflectance of such a system irradiated from the substrate/film interface side can differ by as much as 15% from its reflectance given film/air side incidence (see Fig. 1). Moreover, this large asymmetry in reflectance has been found to be extremely broadband, spanning most of the visible frequency spectrum. For comparison, the reflectance asymmetry of thin, *continuous* silver films does not exceed 3% when measured over the same range of optical frequencies and does not exhibit any broadband characteristics. It has been suggested that the origin of this large broadband asymmetry is in the enhanced optical absorbance which is often seen in percolation-type systems. Here we develop a quantitative description of the observed phenomenon.

The geometry of the system described in this paper is shown in Fig. 1. We approximate the silver percolation film as a uniform material with thickness d [in our calculations $d = 50$ nm (see Sec. III)]. The microstructure of the film is characterized by the surface metal filling fraction p ranging from $p = 0$ for a bare glass substrate to $p = 1$ for a substrate which is fully covered with metal. At the critical value $p = p_c$, known as the *percolation threshold*, the dc conductivity response of the entire random metal-dielectric composite undergoes an insulator-conductor phase transition.[12] The unique optical properties of our films are manifest particularly in the vicinity of the percolation threshold. We therefore adopt the conventional description of the response as function of the parameter $p - p_c$ for the purpose of both modeling and data analysis. All theoretical and experimental results in this work use $p_c = 0.6$, which correlates well with two-dimensional site percolation on a square lattice ($p_c \simeq 0.593$).[12]

As mentioned above, the reflectance R_1 of the composite film, measured using light impinging from the air/metal interface, strongly differs from R_2, the reflectance measured when light is incident from the substrate/film side. Since the transmittance of our system, like the transmittance of any nonchiral homogeneous film, is symmetric (i.e., $T_1 = T_2$),[13,14] the asymmetry in reflectance $\Delta R \equiv R_1 - R_2$ directly reflects the asymmetry in losses.[15] As we show below, in contrast to vacuum-deposited percolation films, (i) ΔR as well as the computed combined losses exhibit a local minimum at $p \simeq p_c$, (ii) ΔR exhibits broadband response in the vicinity of $p - p_c \simeq \pm 0.05$, (iii) the reflectance exhibits a local maximum in the vicinity of $p \simeq p_c$, and (iv) the transmittance exhibits a local minimum near $p \simeq p_c$.

II. PERCOLATION FILM SYNTHESIS AND CHARACTERIZATION

Semicontinuous silver films with controllable filling fractions were deposited on microscope slides using a modified Tollen's reaction as described previously.[11,16] The amount of silver deposited on the substrates was controlled by monitoring deposition times, with reactions ranging between 1 and 6 h. Following deposition, coated substrates were rinsed with ultrapure water before being dried with filtered air and stored under nitrogen until tested. Figure 2 shows a scanning electron micrograph of a typical film with filling fraction $p \simeq 0.52$. These chemically deposited films appear as highly disordered polycrystalline aggregates, with large grain size distributions. In addition, we note the nonuniform coating of the substrates by the metal, resulting in highly discontinuous morphologies.

Optical reflectance and transmittance spectra were collected using a spectroscopic optical microscopy setup.[11] A tungsten-halogen white-light source was used to illuminate the samples through an inverted microscope whose output was imaged on the entrance slit of an $F = 320$ mm spectrometer with a resolution of 0.5 nm. A $10\times$ (0.25 numerical aperture) objective was used to collect the normally incident light for spectroscopic imaging onto a liquid-nitrogen-cooled detector. A high-reflectance mirror (Newport Broadband SuperMirror, $R \geqslant 99.9\%$) was used to normalize all signals. In addition,

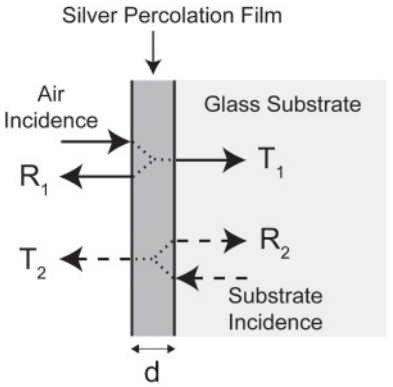

FIG. 1. General layered structure composed of a silver percolation film clad by air to the left and glass to the right. Incident light may come from either the air or substrate side as shown. Both air and glass regions are taken to be semi-infinite.

data from ~1000 μm across the films were averaged to obtain each final trace, in order to eliminate spurious effects from local inhomogeneities in the rough films. The spectral response of the film shown in Fig. 2 is depicted in Fig. 3.

III. REFLECTION, TRANSMISSION, AND ABSORPTION OF RANDOM PERCOLATION COMPOSITES

Many metal-dielectric composite systems are described by effective medium techniques[17–20] (EMTs) by representing the composite as an effective homogeneous layer which successfully models the system's average optical properties. However, it is known that the optical properties of these films close to the percolation threshold cannot be adequately described by EMTs.[21,22] The reason for the consistent failure of EMTs in this case is twofold. First, although the dimensions of the components in percolation films are much smaller than the free-space wavelength, the optical properties of the composites are dominated by the dynamics of resonant clusters that can be comparable in size to the wavelength. Second, as a result of

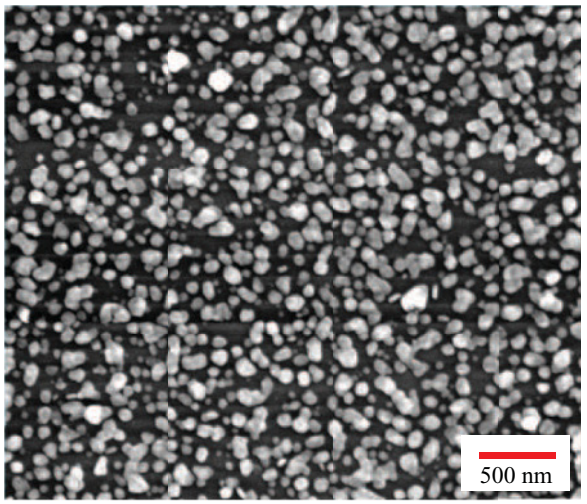

FIG. 2. (Color online) Scanning electron micrograph of a chemically deposited silver film with metal filling fraction $p \simeq 0.52$. The scale bar is 500 nm.

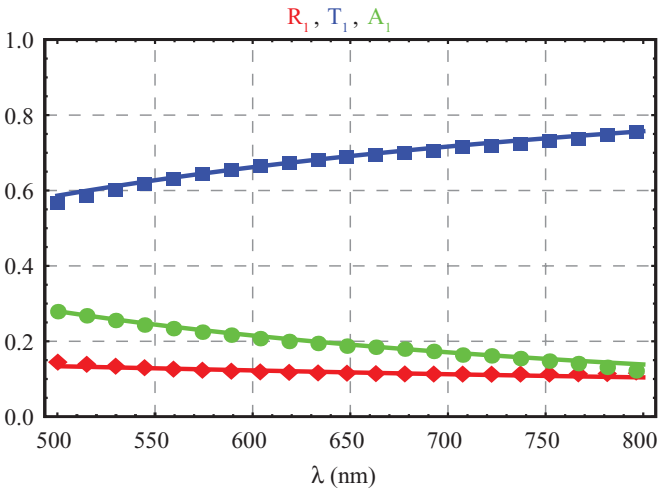

FIG. 3. (Color online) Measured reflectance (red diamonds), transmittance (blue boxes), and absorbance (green circles) as functions of incident wavelength for measured metal filling fraction $p \simeq 0.52$. Solid lines represent the results of scaling theory calculations.

a dc metal-dielectric phase transition, the effective parameters of the percolation films in the vicinity of p_c become scale dependent and therefore cannot be described by quasistatic effective medium models. Although some percolation films have been successfully described in terms of a generalized Ohm's law (GOL),[23–25] straightforward extensions of the GOL formalism to our system are not consistent with our experimental observations.

The only technique that explicitly accounts for the dc conductivity phase transition of percolation systems is known as *scaling theory*.[21,22,26–28] In this technique, the conductivity of the film is assumed to be explicitly dependent on the size of the cluster, L, over which it is measured. Specifically, the average conductivity of a conductive cluster of size L is given by

$$\sigma_m(L) = \frac{C_1\sigma_{dc}}{1+\omega^2\tau^2}\left(\frac{L}{\xi_0}\right)^{-\mu/\nu} + i\left[\frac{C_1\sigma_{dc}\omega\tau}{1+\omega^2\tau^2}\left(\frac{L}{\xi_0}\right)^{-\mu/\nu} - C_2\omega C_0\left(\frac{L}{\xi_0}\right)^{s/\nu}\right], \quad (1)$$

and that of a dielectric (insulating) cluster is

$$\sigma_d(L) = \frac{C_3\omega^2C_0^2}{\sigma_{dc}}\left(\frac{L}{\xi_0}\right)^{(\mu+2s)/\nu} + i\left[\frac{C_3\omega^2C_0^2\omega\tau}{\sigma_{dc}}\left(\frac{L}{\xi_0}\right)^{(\mu+2s)/\nu} - C_4\omega C_0\left(\frac{L}{\xi_0}\right)^{s/\nu}\right]. \quad (2)$$

The expressions above explicitly assume that the conductivity of the conductive component of the film is given by the Drude model,

$$\sigma_1 = \frac{\sigma_{dc}}{1-i\omega\tau}, \quad (3)$$

where σ_{dc} is the dc conductivity, τ is the electron relaxation time, and ω is the angular frequency of the incident light. The

ac response of a dielectric film component is equivalent to that of a capacitor,

$$\sigma_2 = -i\omega C_0, \tag{4}$$

where C_0 is the average capacitance between neighboring metal clusters. The parameters σ_{dc}, τ, ξ_0, C_0, and the $C_1, \ldots, C_4$ coefficients are uniquely determined by the composition and microgeometry of the percolation film. The critical exponents for two-dimensional (2D) percolating films are $\mu \simeq s \simeq \nu \simeq 4/3$.[21,22,29] For $p \ll p_c$, percolation films are governed by dielectric conductivity, which is dominated by the capacitance coefficients C_3 and C_4. For $p \gg p_c$, metallic conductivity (governed by C_1 and C_2) dominates the optical properties of the system.

Despite the scale dependence on the microscopic and mesoscopic levels, the percolation film appears homogeneous when measured over a significantly large area. The transition from the scale-dependent to the homogeneous dc response occurs at the scale known as the *correlation length* ξ, which characterizes the typical cluster size. In the vicinity of the percolation threshold, the correlation length diverges as

$$\xi = \xi_0 \left| \frac{p - p_c}{p_c} \right|^{-\nu}. \tag{5}$$

The constant ξ_0 represents the smallest metal cluster size, which occurs at $p \to 0$.

At finite frequencies, the oscillatory motion of electrons within conducting clusters leads to a finite correlation length, which is the length scale where the percolation film behaves as homogeneous material,

$$L(\lambda_0) = \min \begin{cases} B_0 \xi_0 \left(\lambda_0 / 2\pi \xi_0\right)^{1/(2+\theta)}, \\ \xi(p), \end{cases} \tag{6}$$

where $\theta = 0.79$, $B_0 = 4.0$, and the free space wavelength is given by λ_0.[21,22]

The ac conductivity of the percolation films, calculated using the expressions above, can be directly related to an effective film index, which along with the film thickness d can be used to determine the macroscopic optical properties of the film, including R and T. In our calculations, we use the technique introduced in Ref. 21. In this approach, the optical properties of the film are calculated as a weighted average of conductive (dielectric) film contributions, where the average conductivities are given by Eqs. (1) and (2), respectively, to yield

$$T = \int_0^\infty [f T_\sigma(z\sigma_m) + (1 - f) T_\sigma(z\sigma_d)] P(z) dz, \tag{7}$$

$$R_i = \int_0^\infty [f R_{i,\sigma}(z\sigma_m) + (1 - f) R_{i,\sigma}(z\sigma_d)] P(z) dz, \tag{8}$$

where the parameter

$$f = \frac{1}{2}\left[1 + \left(\frac{p - p_c}{p_c}\right)\left(\frac{L}{\xi_0}\right)^{1/\nu}\right] \tag{9}$$

is the metal occupation probability. For small surface metal concentrations, $p < p_c[1 - (L/\xi_0)^{-1/\nu}]$, the occupation probability $f \to 0$. When $p > p_c[1 + (L/\xi_0)^{-1/\nu}]$ the occupation probability $f \to 1$. For intermediate surface metal concentrations centered at $p = p_c$ with full width $\Delta p = 2p_c(L/\xi_0)^{-1/\nu}$, the occupation probability varies linearly as a function of p from unoccupied ($f = 0$) to occupied ($f = 1$). As shown by the above inequalities, the range of metal surface coverage values for which scaled metal and dielectric optical properties are averaged depends nontrivially on the correlation length, applied frequency, and film geometry. The function $P(z)$ gives the distribution of the conductivities of conductive [dielectric] clusters around their mean values given by Eq. (1) [Eq. (2)]. Following Refs. 21 and 30, we assume that $P(z)$ is adequately described by a log-normal distribution function with standard deviation of $\sigma_{sd} = 0.3$. Integration over all scaled conductivities averages out the length-dependent optical conductivity and allows for percolation films to be modeled by the contributions from planar homogeneous constituent layers.

The homogeneous-layer optical properties are given by[31]

$$T_\sigma = \left| \frac{4 n_f \sqrt{n_s} \Phi}{(1 + n_f)(n_f + n_s) + (1 - n_f)(n_f - n_s)\Phi^2} \right|^2, \tag{10}$$

$$R_{1,\sigma} = \left| \frac{(1 - n_f)(n_f + n_s) + (n_f - n_s)(1 + n_f)\Phi^2}{(1 + n_f)(n_f + n_s) + (1 - n_f)(n_f - n_s)\Phi^2} \right|^2, \tag{11}$$

$$R_{2,\sigma} = \left| \frac{(n_f - n_s)(1 + n_f) + (1 - n_f)(n_f + n_s)\Phi^2}{(1 + n_f)(n_f + n_s) + (1 - n_f)(n_f - n_s)\Phi^2} \right|^2, \tag{12}$$

where the glass substrate index is $n_s = 1.5166$, the effective film index is $n_f = \sqrt{1 + 4\pi i \sigma/\omega}$, and the phase parameter is $\Phi = \exp(i \frac{\omega}{c} n_f d)$.

As noted, all critical exponents in the expressions above are universal for all 2D percolating networks, while the parameters $C_0, \ldots, C_4$, σ_{dc}, τ, and ξ_0 are unique for a given percolation film.[21,22] In our calculations, we use $\sigma_{dc} = 2.574 \times 10^{17}$ s^{-1}, the frequency-dependent relaxation time[32] $1/\tau = 1/\tau_0 + \beta\omega^2$, where $\tau_0 = 3.0$ fs and $\beta = 0.2$ fs, $C_0 = 0.5$, $C_1 = C_2 = 0.046, C_3 = 0.028, C_4 = 0.055$, and $\xi_0 = 2$ nm.

IV. COMPARISON WITH EXPERIMENTAL RESULTS AND DISCUSSION

A comparison of the experimentally obtained spectral response of the silver films with the predictions of scaling theory is shown in Fig. 3. It is seen that both the broadband nature of the reflectance asymmetry and its nonmonotonic behavior near the percolation threshold are well reproduced by the theoretical model, as demonstrated in Fig. 4. We note, however, that the model fails for large metal concentrations $p \to 1$,[11,16] where the structure of the composite becomes substantially three dimensional and it cannot be treated as a thin homogeneous film. To further illustrate the robustness of the presented technique we show in Fig. 5 a comparison of experimentally measured values of R_1 and T_1, as well as the losses (computed as $A_1 = 1 - R_1 - T_1$), with our theoretical model. As mentioned before, both theoretical and experimental results clearly show that, despite a strong reflectance asymmetry, the transmittance of the films remains symmetric. Therefore the asymmetry in reflectance is directly related to the asymmetry in losses ($\Delta R = R_1 - R_2 = A_2 - A_1$).[11]

We now examine the loss (or, alternately, the reflectance) in more detail. We note that several previous experiments as well

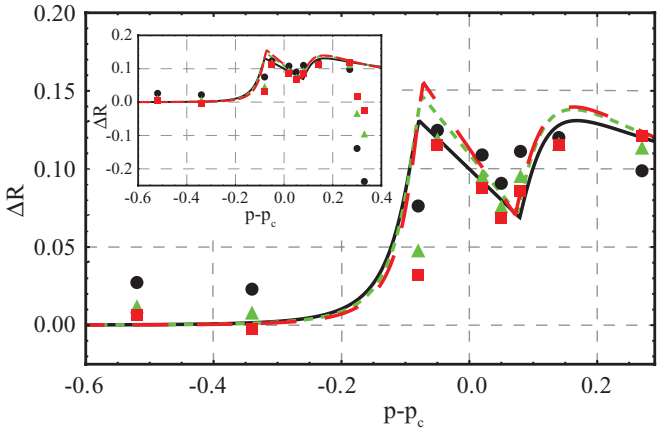

FIG. 4. (Color online) Reflectance asymmetry in solution-derived percolation films. Points represent the measured change in reflectance ($\Delta R = R_1 - R_2$) for various incident wavelengths. Black circles, 500 nm; green triangles, 600 nm; red boxes, 700 nm. Corresponding colored solid lines (black solid, 500 nm; green short dashed, 600 nm; red long dashed, 700 nm) represent the results of scaling theory reflectance calculations. The inset shows the change in reflectance over the entire surface coverage range. Note that the 2D scaling model fails for large metal concentrations, where the three-dimensional structure of the composite dominates the optical response.

as theoretical models have observed absorption maxima in the vicinity of $p = p_c$. In contrast, our experimental data clearly demonstrate a local *minimum* in losses near the percolation threshold, as seen in Fig. 5(e). Additionally we observe a local *maximum* in reflectance and a local *minimum* in transmittance near $p = p_c$, as seen in Figs. 5(a) and 5(c).

We suggest that this anomalous behavior stems from the dramatically reduced correlation length in our solution-derived percolation films. The smallest metallic particle size produced in our experiments is on the order of 2 nm, in contrast to 10 nm reported in Ref. 22. In addition, the optical response of solution-derived metals is typically affected by the reduced electron mean free path,[33] which may further reduce the effective particle size, described by the parameter ξ_0.

Figure 5 demonstrates the evolution of optical properties of percolation systems when the correlation length is reduced, corresponding to a change in ξ_0 from 10 to 2 nm. It is clearly seen that at $\xi_0 \simeq 2$ nm the absorption reaches a local minimum in the vicinity of $p = p_c$, while at $\xi_0 = 10$ nm, the system recovers the absorption maximum at $p = p_c$, as observed in previous studies.

The dramatic difference between correlation lengths in our solution-derived films[11,16] and other vacuum-deposited counterparts[21,23,34] is consistent with the difference in fabrication techniques: while thermal deposition under vacuum typically yields uniform metal films with almost perfect Ohmic contacts between adjacent grains, solution-based deposition is routinely associated with quantitatively weaker contacts

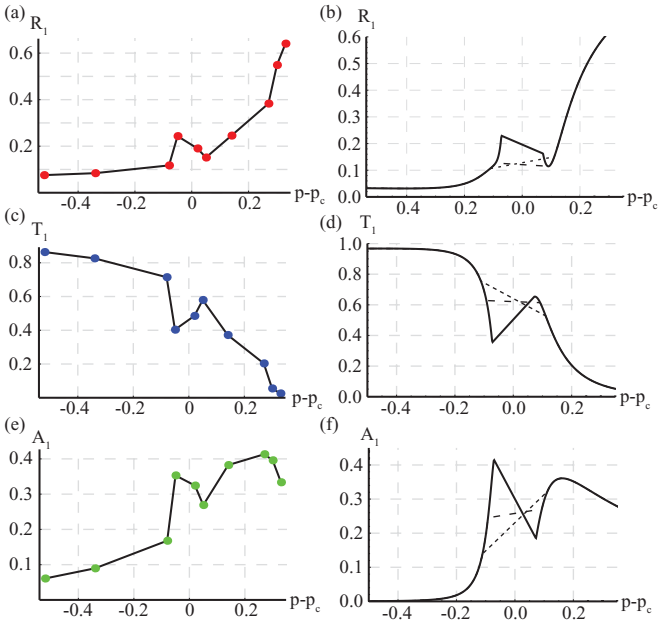

FIG. 5. (Color online) Dependence of the percolation film optical properties on the correlation length. Points represent the measured (a) reflectance, (c) transmittance, and (e) loss from the air side as functions of surface coverage fraction. Connecting lines are a guide for the eye. Calculated (b) reflectance, (d) transmittance, and (f) loss when the correlation length parameter is $\xi_0 = 2$ nm (solid line), $\xi_0 = 5$ nm (dashed line), and $\xi_0 = 10$ nm (dotted line). For all graphs the incident wavelength is 700 nm.

between conducting grains. The latter results in films with reduced electron mean free paths and lower correlation lengths.

V. CONCLUSION

We have developed an analytical description of the phenomenon of broadband asymmetric reflection in percolation composites. The technique developed, based on scaling theory, not only is capable of describing the spectral response of our films, but also explains that the reduced correlation length in our solution-derived composites is the primary cause of the experimentally observed anomalous optical properties near the percolation threshold. Our work demonstrates that the correlation length is an important factor that fundamentally affects the optical properties of percolation composites in the vicinity of the percolation threshold.

ACKNOWLEDGMENTS

This research is sponsored in part by ONR (Grant No. N00014-07-1-0457), NSF (Grants No. ECCS-0724763, No. DMR-02-39273, and No. DMR-08-04433), and PRF (Grant No. 43924-G10).

*kuhtan@onid.orst.edu
†Material Science Division, Argonne National Laboratory, Argonne, IL 60439, USA.
‡Laboratory of Cellular and Molecular Biology, National Cancer Institute, NIH, Bethesda, MD 20892-4256, USA.
§miriamd@uoregon.edu

‖viktor_podolskiy@uml.edu

[1]M. I. Stockman, S. V. Faleev, and D. J. Bergman, Phys. Rev. Lett. **87**, 167401 (2001).
[2]D. A. Genov, A. K. Sarychev, and V. M. Shalaev, Phys. Rev. E **67**, 056611 (2003).
[3]A. K. Sarychev, V. A. Shubin, and V. M. Shalaev, Phys. Rev. B **60**, 16389 (1999).
[4]A. K. Sarychev and V. M. Shalaev, Phys. Rep. **335**, 275 (2000).
[5]V. M. Shalaev and A. K. Sarychev, Phys. Rev. B **57**, 13265 (1998).
[6]V. P. Drachev, W. D. Bragg, V. A. Podolskiy, V. P. Safonov, W. T. Kim, Z. C. Ying, R. L. Armstrong, and V. M. Shalaev, J. Opt. Soc. Am. B **18**, 1896 (2001).
[7]A. Lagarkov, K. Rozanov, A. Sarychev, and N. Simonov, Physica A **241**, 199 (1997).
[8]V. M. Shalaev, *Optical Properties of Nanostructured Random Media*, 1st ed. (Springer, Berlin, 2002).
[9]M. I. Stockman, Phys. Rev. Lett. **84**, 1011 (2000).
[10]M. I. Stockman, L. N. Pandey, L. S. Muratov, and T. F. George, Phys. Rev. Lett. **72**, 2486 (1994).
[11]A. Chen, K. Hasegawa, V. A. Podolskiy, and M. Deutsch, Opt. Lett. **32**, 1770 (2007).
[12]D. Stauffer and A. Aharony, *Introduction to Percolation Theory*, 2nd ed. (Taylor & Francis, London, 1992).
[13]L. D. Barron, *Molecular Light Scattering and Optical Activity*, 2nd ed. (Cambridge University Press, Cambridge, 2004).
[14]V. A. Fedotov, P. L. Mladyonov, S. L. Prosvirnin, A. V. Rogacheva, Y. Chen, and N. I. Zheludev, Phys. Rev. Lett. **97**, 167401 (2006).
[15]Since the model we use here utilizes a uniform smooth film of known thickness, standard boundary conditions allow only specular reflection to occur. We therefore employ the common approach which does not distinguish between specular and diffuse loss mechanisms (Ref. 21), lumping them together into a *generalized combined loss*.
[16]M. S. M. Peterson and M. Deutsch, J. Appl. Phys. **106**, 063722 (2009).
[17]J. C. Maxwell Garnett, Philos. Trans. R. Soc. London, Ser. A **203**, 385 (1904).
[18]D. A. G. Bruggeman, Ann. Phys. (Leipzig) **24**, 636 (1935).
[19]G. W. Milton, *The Theory of Composites*, 1st ed. (Cambridge University Press, Cambridge, 2002).
[20]M. A. Noginov and V. A. Podolskiy, *Tutorials in Metamaterials*, 1st ed. (CRC, Boca Raton, FL, 2011).
[21]Y. Yagil, M. Yosefin, D. J. Bergman, G. Deutscher, and P. Gadenne, Phys. Rev. B **43**, 11342 (1991).
[22]Y. Yagil, P. Gadenne, C. Julien, and G. Deutscher, Phys. Rev. B **46**, 2503 (1992).
[23]A. K. Sarychev, D. J. Bergman, and Y. Yagil, Phys. Rev. B **51**, 5366 (1995).
[24]R. Levy-Nathansohn and D. J. Bergman, Physica A **241**, 166 (1997).
[25]R. Levy-Nathansohn and D. J. Bergman, Phys. Rev. B **55**, 5425 (1997).
[26]J. P. Straley, J. Phys. C **9**, 783 (1976).
[27]Y. Gefen, A. Aharony, and S. Alexander, Phys. Rev. Lett. **50**, 77 (1983).
[28]M. Imada, A. Fujimori, and Y. Tokura, Rev. Mod. Phys. **70**, 1039 (1998).
[29]C. A. Rohde, K. Hasegawa, and M. Deutsch, Phys. Rev. Lett. **96**, 045503 (2006).
[30]R. Rammal, M. A. Lemieux, and A. M. S. Tremblay, Phys. Rev. Lett. **54**, 1087 (1985).
[31]J. R. Reitz, F. J. Milford, and R. W. Christy, *Foundations of Electromagnetic Theory*, 4th ed. (Addison-Wesley, Reading, MA, 1993).
[32]M. L. Theye, Phys. Rev. B **2**, 3060 (1970).
[33]P. H. Lisseberger and R. G. Nelson, Thin Solid Films **21**, 159 (1974).
[34]P. Gadenne, Y. Yagil, and G. Deutscher, J. Appl. Phys. **66**, 3019 (1989).